Exploring the Tilt-Angle Dependence of Electron Tunneling across Molecular Junctions of Self-Assembled Alkanethiols

T. Frederiksen,[†,]* C. Munuera,[‡] C. Ocal,[‡] M. Brandbyge,[§] M. Paulsson,[⊥] D. Sanchez-Portal,[†,¶] and A. Arnau[†,¶,#]

[†]Donostia International Physics Center (DIPC), Paseo Manuel de Lardizabal 4, San Sebastián 20018, Spain, [‡]Institut de Ciència de Materials de Barcelona, CSIC, Bellaterra 08193, Spain, [§]DTU Nanotech, NanoDTU, Technical University of Denmark, 2800 Lyngby, Denmark, [⊥]School of Pure and Applied Natural Sciences, University of Kalmar, 391 82 Kalmar, Sweden, [¶]Centro de Física de Materiales CFM-MPC, Centro Mixto CSIC-UPV, Apdo. 1072, San Sebastián 20080, Spain, and [#]Departamento Física de Materiales UPV/EHU, Facultad de Química, Apdo. 1072, San Sebastián 20080, Spain

ABSTRACT Electronic transport mechanisms in molecular junctions are investigated by a combination of first-principles calculations and current−voltage measurements of several well-characterized structures. We study self-assembled layers of alkanethiols grown on Au(111) and form tunnel junctions by contacting the molecular layers with the tip of a conductive force microscope. Measurements done under low-load conditions permit us to obtain reliable tilt-angle and molecular length dependencies of the low-bias conductance through the alkanethiol layers. The observed dependence on tilt-angle is stronger for the longer molecular chains. Our calculations confirm the observed trends and explain them as a result of two mechanisms, namely, a previously proposed intermolecular tunneling enhancement as well as a hitherto overlooked tilt-dependent molecular gate effect.

KEYWORDS: molecular junctions · alkanethiols · self-assembled monolayers · conducting scanning force microscopy · first-principles transport calculations

Comprehension and control of electron transport through organic molecules are actively pursued in both basic and applied research.[1,2] Fundamental to these goals is a detailed determination of the structure under investigation at the molecular level. Even in cases where molecular films grown on metallic surfaces are well characterized, the interface between the molecules and the electrodes is generally uncertain. In principle, measurements with single-molecule junctions could permit a better characterization of the contacts, as recent data seem to indicate.[3−5] However, even this type of junctions is difficult to control and characterize experimentally. Thus, to obtain a complete understanding of transport through molecular junctions, it is crucial to consider and compare experiments to theories taking into account the atomic details. In this context, the information gained from first-principles calculations can be of great help.[5−8]

Self-assembled monolayers (SAMs) of alkanethiols grown on Au(111) have become a prototype system for experimental testbeds in molecular electronics.[7−17] Although the first electrical measurements on alkane-based SAMs were performed more than three decades ago,[18] there is a considerable ongoing activity pursuing the characterization of electronic transport across the junctions at the microscopic scale.[19,20] As the highest occupied molecular orbital (HOMO) and the lowest unoccupied molecular orbital (LUMO) are far away from the Fermi level (E_F) of the electrodes [within the present treatment based on density functional theory (see Methods Section), the calculated gap for the infinite alkane chain is

of the order of 8 eV] the electronic transport across these molecular films takes place in the nonresonant tunneling regime. At low and intermediate bias, compared to the tunnel barrier height, the Simmons model[21] has been widely used to extract parameters, like barrier heights and inverse decay lengths. However, its applicability is not fully justified, as it is based on a purely one-dimensional trapezoidal tunneling barrier combined with semiclassical (WKB) transmission functions. Recently, Wang et al.[16] have used a three barrier model with fitting parameters to study the influence of the metal−molecule contact on the junction conductivity for both alkanethiols and alkanedithiols. Furthermore, the fact that the organic overlayer is highly anisotropic obviously requires special attention, as can be concluded by the failure of descriptions based on a continuous dielectric model to represent it.[22]

It is anticipated that the conductance of metal−alkanethiol−metal junctions

*Address correspondence to thomas_frederiksen@ehu.es.
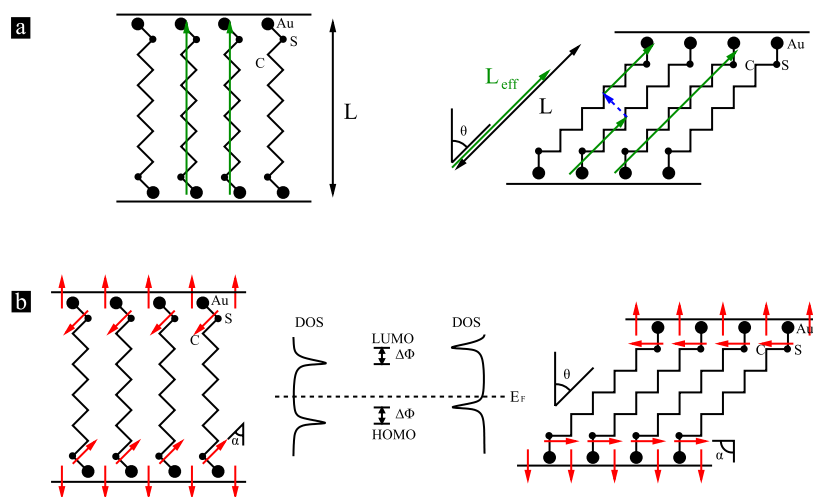
© 2009 American Chemical Society

Figure 1. Schematic of the two important tunneling enhancement mechanisms in tilted alkanethiol SAMs. The molecular tilt angle θ and S−C bond angle α are defined with respect to the surface normal. (a) The first mechanism is based on the geometry of the tunneling pathway, which is commonly separated into intramolecular (through-bond) and intermolecular (through-space) contributions. These two generic pathways are illustrated with green and blue/dashed arrows, respectively. As indicated for the tilted SAM, a tunneling electron can shorten its effective path along the molecular backbone at the price of tunneling to the neighboring molecule. This opens up an additional tunneling pathway which can enhance the overall tunneling probability. (b) The other mechanism, which we denote the tilt-dependent molecular gate effect, arises from changes in the effective interface dipole (vector sum of the red arrows), which has contributions from a permanent surface dipole and a molecular dipole oriented along the S−C bond (characterized by the angle α). When the molecules are tilted by θ, the effective dipole is reduced and the work function of the decorated surface increases. As sketched, this results in an upward shift of the molecular orbitals with respect to the Fermi energy, and hence in enhanced tunneling through the tail of the HOMO resonance.

depends on the geometry of the molecular arrangement, in particular on the tilt angle θ that characterizes the alignment of the SAM with respect to the surface normal. By applying a force to the molecular film with the tip of a scanning force microscope (SFM), it has been established that tunneling through alkanethiol SAMs increases with applied load.[8,15,23] This dependence has been assigned to the tilt configuration, despite that film compression may induce gauche defects and changes in the nature of the Au−S bond, which complicate the interpretation of experimental data.[6]

Within an extension of the Simmons model, a common approach to understand the tilt dependence of tunneling in alkanethiol SAMs is based on two different contributions, an intramolecular (through-bond) and an intermolecular (through-space).[22] This picture is illustrated in Figure 1a. Direct tunneling between electrodes can safely be ignored because such contributions are several orders of magnitude smaller.[24] Despite many efforts to quantify these intra- and intermolecular contributions, no conclusive picture has yet emerged, neither have alternative mechanisms been proposed to explain the experimental trends.

In the present study, we make use of our ability to grow and prepare differently tilted molecular configurations[25] for various lengths of methyl-terminated alkanethiol molecules [$CH_3(CH_2)_{n-1}SH$, referred to as Cn from now

on]. To ensure essentially no film deformation our conducting SFM (C-SFM), experiments were always performed at the lowest practical load. Our approach provides well-characterized, highly ordered molecular films to establish comparative analysis, which helps overcoming the otherwise general lack of tip-film contact description in any C-SFM investigations. We observe that the conductance of alkanethiol junctions are higher for the more tilted configurations and that this increase is more pronounced for the longer molecular chains. Using first-principles methods we are able to describe the elastic transport mechanisms at the molecular level comparing the trends of calculated and measured conductance values. Our simulations indicate that the observed conductance behavior can be related to intermolecular contributions *and* to a tilt-dependent molecular gate effect. The latter mechanism, which so far has been overlooked, arises from the change of effective interface dipole with variations in the molecule−substrate bonding geometry. Specifically, when thiol groups are tilted with respect to the metal, the work function of the decorated surface increases. As a consequence, the molecular levels shift upward with respect to the Fermi level in the contacts, thereby enhancing tunneling through the tail of the HOMO resonance (see Figure 1b).

EXPERIMENTAL RESULTS

Islands of self-assembled molecules on Au(111) substrates were prepared following the procedure described elsewhere.[25] This procedure leads to the formation of alkylthiol islands, presenting two differently tilted configurations of upright molecules. These two structures and their molecular orders, the hexagonal ($\sqrt{3} \times \sqrt{3}$)R30° of the monolayer and a rectangular (2 $\times \sqrt{3}$)rect phase, have already been reported.[12,25] The molecules are tilted by θ = 30° and θ = 50° from the surface normal, and their packing areas correspond to 21.6 Å² and 28.7 Å² per molecule, respectively. Additional advantages of using submonolayer coverages are (i) ordered single domains are obtained, which are larger in size and better in crystalline quality than those obtained for complete monolayers even after annealing; (ii) the bare gold serves as an *in situ* reference for lattice periodicity determination and transport response.

As commented above, this ability to obtain differently tilted configurations for the same molecular length offers an elegant way to investigate the electronic transport through these layers by establishing

comparative analysis while avoiding film compression (see Methods Section).

Figure 2a,b shows an example of simultaneous topographic and current C-SFM images of a sample consisting of C12 islands partially covering the gold substrate terraces. These images are acquired in contact mode at the lowest practical load (the pull-off force) to avoid compression of the organic layers while providing precise film thickness.[12] Topographic profiles and high resolution imaging (not shown) were acquired to confirm the actual structure (tilt and molecular order). Because of the different electrical character of the metallic bare gold and the poorly conducting alkanethiol molecules, the C12 islands are easily identified as black patches in this low-voltage current image.

Figure 2c shows typical $I-V$ curves measured on top of both 30° and 50° tilted configurations. The characteristic sigmoidal shape reported for alkanethiol junctions, and shown here for the case of C12, was always observed over the ± 2 V for both structures and the three molecular lengths investigated. It is more clearly visualized for the $\theta = 50°$ case (in red), which for a given voltage yielded higher current values as compared to the $\theta = 30°$ case (in black). The linear response of the $I-V$ curves around the low bias region (± 0.5 V) (see inset) were used to estimate the experimental resistances (defined as the inverse slope) of the corresponding molecular junction.

Using the experimental procedure described above, we obtained the junction resistance for six different layer thicknesses, namely for C12, C16, and C18 alkanethiol islands exhibiting each of the two characteristic tilt angles. To minimize any tip-dependent effects, the same conducting probe has been used for the whole experimental data summarized in Table 1, which facilitates the analysis of the results and the comparison between measurements and calculations.

In Table 1 we also present the relative conductance ratios as θ changes from 30° to 50°, being aware of the fact that the two different structures correspond to slightly different molecular coverages. From the measured $I-V$ characteristics and using reasonable values of the effective contact area,[17] we can estimate values for the single-molecule conductances. For C12 we estimate it to be in the range 10^{-7} to 10^{-6} G_0, where G_0 is the conductance quantum.

Here, we are mainly interested in relative changes of the junction conductance as a function of the tilt angle θ and length of the C backbone. The essential
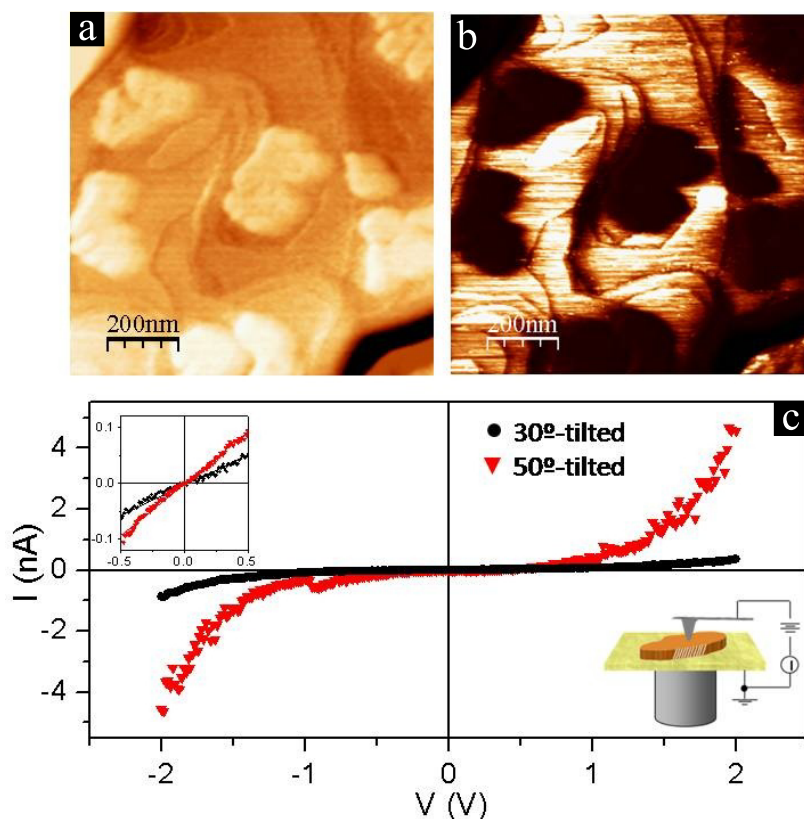
Figure 2. (a,b) Simultaneous SFM topographic (left) and current (right) images acquired at a tip voltage of 300 mV on a sample exhibiting C12 islands. The corresponding color codes are such that the total vertical scales are 0−7 nm for panel a and 0−15 nA for panel b. (c) Current−voltage ($I-V$) curves for C12 islands presenting the $\theta = 30°$ and $\theta = 50°$ tilted configurations. Insets show the $I-V$ data over ± 0.5 V (top left) used to estimate the experimental junction resistances and the C-SFM setup schematics (bottom right).

trends to notice from Table 1 are (i) the junction conductance increases with θ and (ii) the conductance increase grows with the length of the molecule. These results cannot be solely explained by a reduced electrode separation and calls for modeling that takes into account the structural and chemical details of the SAMs.

THEORETICAL RESULTS

We have carried out first-principles transport calculations for a series of SAM geometries varying both the tilt angle and C-backbone length. Specifically, we use a supercell representation of the junctions including a single alkanedithiol molecule connected to two Au(111) electrodes via Au-adatoms on hollow sites, corresponding to an hexagonal packing geometry, as shown in Figure 3. The molecular coverage is throughout these calculations kept fixed at one molecule per surface unit cell in a p-2 × 2 symmetry on the Au(111) surface plane

TABLE 1. Measured Junction Resistances R (in GΩ) as a Function of Alkane Backbone Length and Tilt Angle θ (in deg)

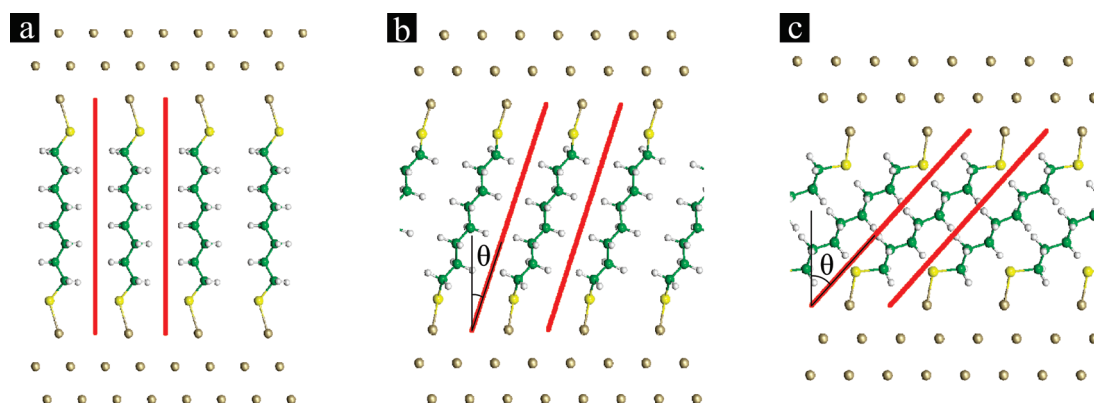| tilt angle θ	R (C12)	R (C16)	R (C18)
30	1.3×10^2	2.5×10^3	2.08×10^4
50	6.5×10^1	3.3×10^2	1.7×10^3
ratio	2.0	7.6	12.2

Figure 3. View of three geometries used in our first-principles calculations for C8 molecules between Au(111) surfaces. The nominal tilt angle θ corresponds to 0°, 30°, and 50°, in panels a, b, and c, respectively.

(*i.e.*, an area of 30.3 Å^2 per molecule), except for obtaining the results presented in Table 2, where a p-4 × 4 symmetry with four times lower coverage, has also been used.

The junction geometries considered in the calculations deviate in certain aspects from the experimental situation (see Methods Section). On the one hand, the actual molecular coverage and θ are not independent variables, as the molecular packing is the result of the optimization with respect to the intermolecular van der Waals interactions. The observed configurations have similar packing areas as the ones considered in the calculations, the maximum difference being about 30% for the 30°-tilted structure. Moreover, although the actual packing geometries for θ = 30° and θ = 50° in fact correspond to hexagonal and rectangular molecular orders, respectively, the relevant parameter for our purposes is the chain−chain distance. This distance is around the optimum van der Waals distance (∼4 to 5 Å) in both theory and experiment. On the other hand, our experiments involve monothiol SAMs, that is, molecules are only chemically bonded to one of the electrodes, the Au(111) surface. This fact can easily account for 1 order of magnitude lower conductance than for corresponding dithiol junctions.[19] Furthermore, the experimental average—over different Au−S bonding configurations and molecular end-group contacts to the tip—is likely to further affect the final measured conductance. While it has been shown that the conductance of alkanedithiol junctions can be sensitive to the

Au−S binding site,[26] only binding to Au adatoms are considered here. This choice, motivated in the Methods Section to control the tilt angle, is therefore justified because the experimental Au−S bonding configurations in the tilted SAMs are not fully characterized anyways. Finally, we remark here that our interest is not to reproduce absolute conductance values but to understand the observed trends to infer some general conclusions.

As an example of the elastic electron transport properties of the junctions we show in Figure 4a the transmission function $T(E)$ for C8 at the three different tilt angles. The transmission probability at E_F is of the order 10^{-3}, that is, the vast majority of incoming electron waves at this energy are backscattered at the molecular interface. However, as the figure shows, sufficiently away from E_F the transmission approaches unity (associated with resonant transport). This picture supports the notion that the electron transport through alkanes is off-resonance and through a HOMO−LUMO gap of several eV.

To shed some light on the origin of the features in the transmission function, we have calculated the projected density of states (PDOS) onto the basis orbitals associated with the different species in the junction. This is shown in Figure 4b. Despite some minor changes with θ, the panel illustrates some robust features of the electronic structure: (i) The PDOS onto Au basis orbitals has the most significant contribution below −2 eV. This can be understood as the contributions from the 5d valence electrons. (ii) The PDOS onto H and C basis orbitals reveal a HOMO−LUMO gap of the order 7−8 eV. (iii) The PDOS onto S orbitals display a prominent peak just below E_F. Therefore, the features appearing in the transmission function (Figure 4a) for the tilted molecules around E_F − 0.2 eV can be associated with an S derived resonance.[27,28] We note that this resonance shifts slightly *away* from E_F with tilt and therefore cannot contribute significantly to the experimentally observed conductance increase. Figure 4 panels c and d show, for C8 at θ = 0° and θ = 50°, a real-space

TABLE 2. Calculated Conductance (in Units of the Conductance Quantum G_0) per C8 Molecule at High (Dense) and Low (Dilute) Coverages for Three Different Nominal Tilt Angles (θ, in deg)[a]

Nominal angle θ	G (dense)	G (dilute)
0	3.3×10^{-4}	3.0×10^{-4}
30	4.7×10^{-4}	4.6×10^{-4}
50	7.8×10^{-4}	5.4×10^{-4}

[a]The stronger angle dependence at high coverages is consistent with an increasing role of intermolecular couplings (through-space contribution).
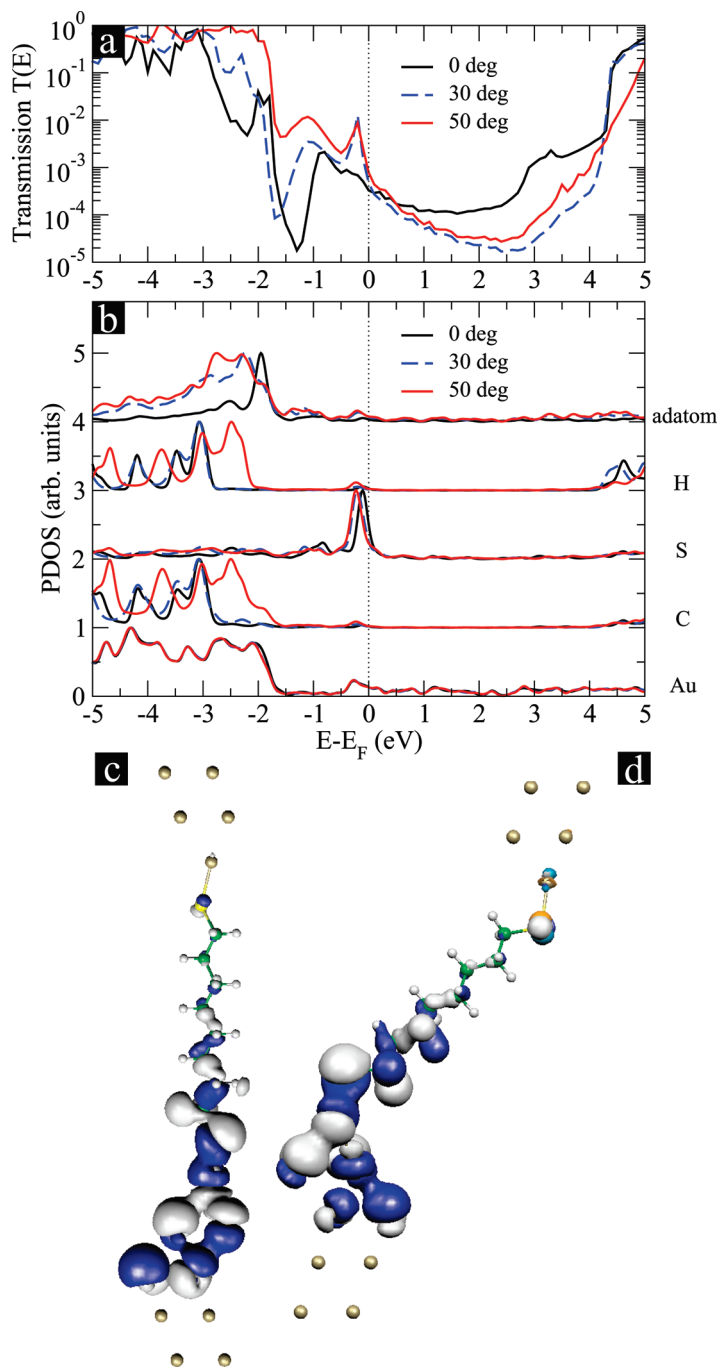
Figure 4. (a) Transmission function $T(E)$ and (b) projected densities of states onto different atoms PDOS(E) as a function of electron energy E for C8 at three different nominal tilt angles θ. (c,d) Real-space distribution of the dominant transmission eigenchannel scattering state at $E = E_F - 0.2$ eV (incoming from below) for C8 molecules at θ = 0° and θ = 50°. The real part is represented in dark blue and white, while the imaginary part in light blue and yellow (the imaginary part is hardly visible because the phase is chosen to be real at the interface at the incoming side). As seen from the scattering state visualization, the transmission resonance at $E_F - 0.2$ eV, observed in panel a for the tilted cases, manifests itself as a phase accumulation on the upper-side electrode S atom in panel d. The electrical current flows from the bottom to the top side Au−S contacts.

representation of the scattering states belonging to the dominant transmission eigenchannel[29] at 0.2 eV below E_F, where the peak in transmission appears. The main difference is that at θ = 50° the scattering state

has relatively more weight on the topmost S atom illustrating that, in this case, the scattering state couples to states localized there, and that a resonance builds up. The corresponding results for C12 molecules are presented in Figure 5. A behavior similar to that for C8 is found for the transmission function and the projected densities of states.

By extracting the transmission values at the Fermi energy we are now in position to theoretically discuss the relative conductance changes with θ. This is shown in Figure 6 for C8 and C12 alkanedithiols. From the computed conductance values we observe that (i) in both cases, the conductance per molecule increases with increasing tilt angle (particularly when going from 30° to 50°), and (ii) the conductance gain at 50° is more pronounced the longer the molecule is. These results fit both with the experimental trends, as well as with the picture of the opening of an intermolecular tunneling pathway for the electrons for the more tilted configuration (see Figure 1a).

To inquire into the contribution from intermolecular tunneling, we have performed calculations for C8 molecules arranged in a larger supercell, namely a 4 × 4. By removing three of the four molecules in this cell we obtain a dilute structure, where the distance between C8 nearest neighbors is two times larger. To keep the interface environment invariant, methanethiols (SCH$_3$) are allocated on the Au adatom positions whenever any C8 molecules were removed from the SAM. In such a way, intermolecular couplings between C8 chains can be considered negligible, while the Au(111) surface has the same chemical termination with respect to Au−S bonds.

Our results for the conductance per molecule in both the dense and dilute C8 structures are presented in Table 2. An increase in conductance with θ occurs for both molecular densities, but—for a given tilt angle—the dilute structure is slightly less conductive. This difference supports the interpretation of an intermolecular contribution in the dense, tilted structures.
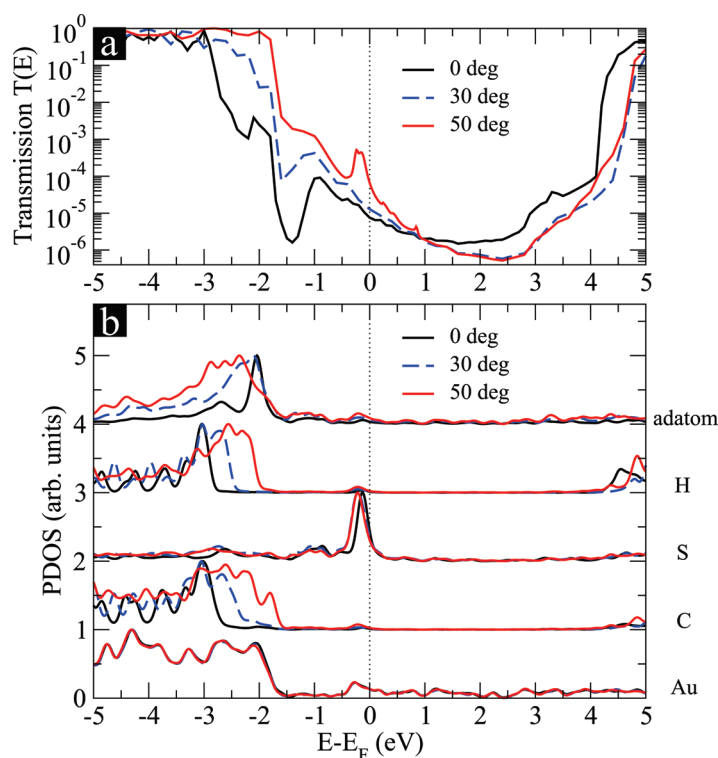
Figure 5. (a) Transmission function and (b) projected densities of states (PDOS) onto different atoms as a function of electron energy for C12 at three different nominal tilt angles (θ).

On the other hand, even the dilute structures display a conductance increase by tilting, despite that the intermolecular contribution should be negligible. We have verified that the general shape of the transmission function as well as the PDOS onto the different basis orbitals were not changed significantly by going from the dense to the dilute structures. This is a good indication that the $AuSCH_3$ termination (with Au adatom, S, and C atoms kept in the equivalent positions as for the bridging molecule) is neither altering the electrostatics nor the electronic structure with respect to the corresponding dense structure.
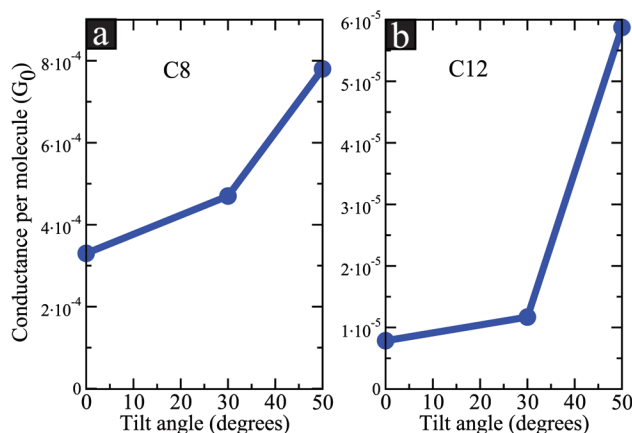
However, from a separate analysis for an $AuSCH_3$ terminated Au(111) surface, we have found that the work function Φ increases by tilting the termination groups.[30−32] This is summarized in Table 3. For instance, with a surface termination derived from C8, the work function is found to increase by 0.08 eV going from $\theta = 0°$ to $\theta = 30°$, and by another 0.76 eV going from $\theta = 30°$ to $\theta = 50°$. These changes can be rationalized by considering the effective interface dipole along the surface normal arising from a permanent surface dipole and a molecular dipole oriented along the S−C bond, as shown in Figure 1. In fact, the changes are well described by a simple $\Delta\Phi = -1.2$ eV cos (α) dependence, where α is the angle of the S−C bond with respect to the surface normal. This result is in good agreement with the reported data in ref 32, once the difference in coverage is taken into account. With this insight we can understand the shifts in PDOS onto C and H orbitals observed in Figure 4 and Figure 5, which simply reflect these modifications in the potential. In other words, when the $AuSCH_3$ groups tilt (thus changing the angle α of the S−C bond), several aspects are affected: the effective interface dipole changes, the surface work function increases, the local electrostatic potential in the molecular gap is modified, the molecular levels shift upward, and—specifically—the HOMO level moves closer to E_F. Consequently, the tunneling through the tail of the HOMO resonance is enhanced. Since the tunneling probability decays exponentially with length and the effective inverse decay length decreases when the molecular level shifts, this tilt-dependent molecular gate effect is therefore *also* consistent with a stronger angle dependence for the longer molecules.

SUMMARY AND CONCLUSIONS

We have employed a combined theoretical and experimental approach to clarify the underlying mechanisms of electronic transport across metal−SAM−metal junctions. The spontaneous formation of structures with different tilt angles, for a given alkanethiol molecular length, has been exploited as a unique tool for accurately investigating the role of well-defined molecular tilt angles. Furthermore, to successfully overcome the assumption of continuous molecular tilting during invasive compression film experiments, C-SFM measurements at the lowest practical load have been performed for different molecular lengths and two different tilt angles (30° and 50°).

Our experimental results permit comparison of conduction properties of molecular junctions with different thickness while essentially preserving the film structure. The data reveal a stronger tilt angle dependence of the conduc-

Figure 6. Theoretically computed conductance per molecule for C8 and C12 for different nominal tilt angles (θ).

TABLE 3. Calculated Relative Increases in the Work Function (in eV) by Different AuSCH$_3$ Terminations of a Perfect Au(111) Surface[a]

	$\Delta\Phi(\alpha)$	
nominal angle θ	C8-type	C12-type
0	0.00 (39)	0.00 (40)
30	0.08 (45)	0.35 (69)
50	0.84 (85)	0.90 (88)

[a]As described in the text, the atomic arrangements of the AuSCH$_3$ groups are derived from the Au—S—C coordinates of the tilted C8 and C12 junctions. As sketched in Figure 1 the changes in work function can be understood by considering the effective interface dipole as resulting from a permanent surface dipole and varying contribution from a molecular dipole oriented along the S—C bond (the angle α between the S—C bonds and the surface normal is shown in deg in the parentheses).

tance for the longer molecules. This trend is reproduced by our first-principles calculations for C8 and C12 molecular layers. To further investigate the importance of intermolecular tunneling pathways, the conductance values for two different C8 structures (low and high coverage) at three different tilt angles have been computed. It was found that the tilt-angle dependence was reduced for the dilute structures, hence suggesting the existence of an intermolecular contribution to the conductance. At the same time, we also found that molecular tilt changes the effective interface dipole and brings the HOMO resonance closer to the Fermi energy. This second mechanism also provides a way for enhancing the conductance with tilt.

To differentiate between the intermolecular tunneling and the molecular gate effect suggested in this study, experimental results for the HOMO level position as a function of tilt angle in alkanethiol SAMs should be pursued. In principle, the proposed level shifts have observable consequences for photoemission and bias spectroscopy. For the studied Au—alkanethiol—Au junctions we have also seen that transport through the HOMO tail is dominating over the LUMO tail. On the basis of the notion that the LUMO is spatially more extended than the HOMO, we further claim that the intermolecular contribution would play a more significant role for LUMO-dominated SAMs.

In summary, we have shown that our combined theoretical and experimental study is a promising route to follow for achieving a microscopic characterization of electronic transport at the molecular level for metal—molecule—metal junctions in general.

METHODS

The experimental procedure is based on the use of C-SFM to simultaneously record topographic and current images as well as to measure $I-V$ characteristics of the molecular junctions under controlled applied load. The complete measuring C-SFM strategy employed has been described in detail elsewhere.[17]

Our theoretical simulations are based on density functional theory as implemented in the SIESTA package.[33] The electronic structure is calculated using a DZP basis set for H, C, and S atoms, and a SZP for the Au atoms and a **k**-point sampling of 2 × 2 × 2. The GGA-PBE[34] functional was used for exchange-correlation, and real-space integrations were performed using a 200 Ry cutoff. For a given geometry, cf. Figure 3, we relax the forces on the molecule and the two Au adatoms until residual forces are smaller than 0.02 eV/Å. The electrode layers (including the two interface layers), described by a bulk gold lattice constant of 4.18 Å, were not relaxed.

The molecular tilt angle θ is modeled by imposing different positions of the Au-adatoms on the Au(111) surfaces, representing the leads, under the constraint of keeping the stretch/length of the molecule approximately constant. Although other possible choices seem reasonable, like bonding S-atoms directly to hollow sites, the Au adatoms are convenient since they function as anchors in well-defined positions on the Au(111) surface (in contrast, a S bond directly on the Au surface will be much more flexible).

In practice, we start by determining the molecular structures for zero tilt angle, and build the tilted geometries by treating the molecule (and adatoms) as a rigid rod that can be connected between different hollow sites on the ideal Au(111) surfaces of the electrodes. As a result of the tilting, the electrodes are brought closer to (approximately) maintain the adatom surface geometry. The geometrically transformed junctions are next relaxed to the force tolerance criteria of 0.02 eV/Å. The resulting geometries are thus only approximately 30° and 50° tilted. The actual angles—defined via the Au adatom coordinates and the surface normal—are 18 (24) and 43 (45) for C8 (C12), respectively.

Having constructed the junction geometries, we determine the corresponding transport properties utilizing the TranSIESTA method.[35] This scheme involves the replacement of periodicity in the transport direction of the supercell description with a matching to semi-infinite atomistic electrodes. The zero-bias conductance per molecule is evaluated from a calculation of the electronic transmission probability at E_F using a 12 × 12 sampling of the two-dimensional Brillouin zone. The use of a dense **k**-point sampling is mandatory to achieve well-converged results.

REFERENCES AND NOTES

1. Aviram, A.; Ratner, M. A. Molecular Rectifiers. *Chem. Phys. Lett.* **1974**, *29*, 277–283.
2. Agrait, N.; Yeyati, A. L.; van Ruitenbeek, J. M. Quantum Properties of Atomic-Sized Conductors. *Phys. Rep.* **2003**, *377*, 81–279.
3. Quek, S. Y.; Venkataraman, L.; Choi, H. J.; Louie, S. G.; Hybertsen, M. S.; Neaton, J. B. Amine-Gold Linked Single-Molecule Circuits: Experiment and Theory. *Nano Lett.* **2007**, *7*, 3477–3482.
4. Hihath, J.; Arroyo, C. R.; Rubio-Bollinger, G.; Tao, N.; Agrait, N. Study of Electron-Phonon Interactions in a Single Molecule Covalently Connected to Two Electrodes. *Nano Lett.* **2008**, *8*, 1673–1678.
5. Quek, S. Y.; Kamenetska, M.; Steigerwald, M. L.; Choi, H. J.; Louie, S. G.; Hybertsen, M. S.; Neaton, J. B.; Venkataraman, L. Mechanically Controlled Binary Conductance Switching of a Single-Molecule Junction. *Nat. Nanotechnol.* **2009**, *4*, 230–234.

6. Paulsson, M.; Krag, C.; Frederiksen, T.; Brandbyge, M. Conductance of Alkanedithiol Single-Molecule Junctions: A Molecular Dynamics Study. *Nano Lett.* **2009**, *9*, 117–121.

7. Li, C.; Pobelov, I.; Wandlowski, T.; Bagrets, A.; Arnold, A.; Evers, F. Charge Transport in Single Au|Alkaneditiol|Au Junctions: Coordination Geometries and Conformational Degrees of Freedom. *J. Am. Chem. Soc.* **2008**, *130*, 318–326.

8. Qi, Y.; Ratera, I.; Park, J. Y.; Ashby, P. D.; Quek, S. Y.; Neaton, J. B.; Salmeron, M. Mechanical and Charge Transport Properties of Alkanethiol Self-Assembled Monolayers on a Au(111) Surface: The Role of Molecular Tilt. *Langmuir* **2008**, *24*, 2219–2223.

9. Munuera, C. Ph.D. Thesis. Universidad Autónoma de Madrid, 2007.

10. Wang, W.; Lee, T.; Reed, M. Mechanism of Electron Conduction in Self-Assembled Alkanethiol Monolayer Devices. *Phys. Rev. B* **2003**, *68*, 035416.

11. Wang, W.; Lee, T.; Reed, M. Electron Tunnelling in Self-Assembled Monolayers. *Rep. Prog. Phys.* **2005**, *68*, 523–544.

12. Barrena, E.; Palacios-Lidon, E.; Munuera, C.; Torrelles, X.; Ferrer, S.; Jonas, U.; Salmeron, M.; Ocal, C. The Role of Intermolecular and Molecule-Substrate Interactions in the Stability of Alkanethiol Nonsaturated Phases on Au(111). *J. Am. Chem. Soc.* **2004**, *126*, 385–395.

13. Wang, R. Y.; Segalman, R. A.; Majumdar, A. Room Temperature Thermal Conductance of Alkanedithiol Self-Assembled Monolayers. *Appl. Phys. Lett.* **2006**, *89*, 173113.

14. Gonzalez, M. T.; Wu, S.; Huber, R.; van der Molen, S. J.; Schoenenberger, C.; Calame, M. Electrical Conductance of Molecular Junctions by a Robust Statistical Analysis. *Nano Lett.* **2006**, *6*, 2238–2242.

15. Song, H.; Lee, H.; Lee, T. Intermolecular Chain-to-Chain Tunneling in Metal−Alkanethiol−Metal Junctions. *J. Am. Chem. Soc.* **2007**, *129*, 3806.

16. Wang, G.; Kim, T.-W.; Lee, H.; Lee, T. Influence of Metal−Molecule Contacts on Decay Coefficients and Specific Contact Resistances in Molecular Junctions. *Phys. Rev. B* **2007**, *76*, 205320.

17. Munuera, C.; Barrena, E.; Ocal, C. Scanning Force Microscopy Three-Dimensional Modes Applied to Conductivity Measurements Through Linear-Chain Organic SAMs. *Nanotechnology* **2007**, *18*, 125505.

18. Mann, B.; Kuhn, H. Tunneling Through Fatty Acid Salt Monolayers. *J. Appl. Phys.* **1971**, *42*, 4398.

19. Akkerman, H. B.; de Boer, B. Electrical Conduction Through Single Molecules and Self-Assembled Monolayers. *J. Phys.: Condens. Matter* **2008**, *20*, 013001.

20. Scaini, D.; Castronovo, M.; Casalis, L.; Scoles, G. Electron Transfer Mediating Properties of Hydrocarbons As a Function of Chain Length: A Differential Scanning Conductive Tip Atomic Force Microscopy Investigation. *ACS Nano* **2008**, *2*, 507–515.

21. Simmons, J. Generalized Formula for Electric Tunnel Effect Between Similar Electrodes Separated By a Thin Insulating Film. *J. Appl. Phys.* **1963**, *34*, 1793.

22. Slowinski, K.; Chamberlain, R.; Miller, C.; Majda, M. Through-Bond and Chain-to-Chain Coupling. Two Pathways in Electron Tunneling Through Liquid Alkanethiol Monolayers on Mercury Electrodes. *J. Am. Chem. Soc.* **1997**, *119*, 11910–11919.

23. Wang, G.; Kim, T.-W.; Jo, G.; Lee, T. Enhancement of Field Emission Transport by Molecular Tilt Configuration in Metal−Molecule−Metal Junctions. *J. Am. Chem. Soc.* **2009**, *131*, 5980–5985.

24. For instance, as reported in ref 8 at a separation of just 6 Å between the electrodes the conductance is 3 orders of magnitude smaller with a vacuum gap than with butaneditiol (C4) molecules. Direct tunneling contributions are thus negligible.

25. Barrena, E.; Ocal, C.; Salmeron, M. Structure and Stability of Tilted-Chain Phases of Alkanethiols on Au(111). *J. Chem. Phys.* **2001**, *114*, 4210–4214.

26. Muller, K. Effect of the Atomic Configuration of Gold Electrodes on the Electrical Conduction of Alkanedithiol Molecules. *Phys. Rev. B* **2006**, *73*, 045403.

27. Kaun, C.; Guo, H. Resistance of Alkanethiol Molecular Wires. *Nano Lett.* **2003**, *3*, 1521–1525.

28. Kim, Y.-H. Toward Numerically Accurate First-Principles Calculations of Nano-Device Charge Transport Characteristics: The Case of Alkane Single-Molecule Junctions. *J. Korean Phys. Soc.* **2008**, *52*, 1181–1186.

29. Paulsson, M.; Brandbyge, M. Transmission Eigenchannels From Nonequilibrium Green's Functions. *Phys. Rev. B* **2007**, *76*, 115117.

30. De Renzi, V.; Rousseau, R.; Marchetto, D.; Biagi, R.; Scandolo, S.; del Pennino1, U. Metal Work-Function Changes Induced by Organic Adsorbates: A Combined Experimental and Theoretical Study. *Phys. Rev. Lett.* **2005**, *95*, 046804.

31. Rousseau, R.; De Renzi, V.; Mazzarello, R.; Marchetto, D.; Biagi, R.; Scandolo, S.; del Pennino1, U. Interfacial Electrostatics of Self-Assembled Monolayers of Alkane Thiolates on Au(111): Work Function Modification and Molecular Level Alignments. *J. Phys. Chem. B* **2006**, *110*, 10862–10872.

32. Nagoya, A.; Morikawa, Y. Adsorption States of Methylthiolate on the Au(111) Surface. *J. Phys.: Condens. Matter* **2007**, *19*, 365245.

33. Soler, J. M.; Artacho, E.; Gale, J. D.; Garcia, A.; Junquera, J.; Ordejon, P.; Sanchez-Portal, D. The SIESTA Method for Ab Initio Order-N Materials Simulation. *J. Phys.: Condens. Matter* **2002**, *14*, 2745–2779.

34. Perdew, J. P.; Burke, K.; Ernzerhof, M. Generalized Gradient Approximation Made Simple. *Phys. Rev. Lett.* **1996**, *77*, 3865–3868.

35. Brandbyge, M.; Mozos, J. L.; Ordejon, P.; Taylor, J.; Stokbro, K. Density-Functional Method for Nonequilibrium Electron Transport. *Phys. Rev. B* **2002**, *65*, 165401.